JOURNAL OF CATALYSIS **161,** 730–741 (1996)
ARTICLE NO. 0235

Dehydrogenation of Isobutane over Zinc Titanate Thin Film Catalysts

Z. X. Chen,* A. Derking, W. Koot, and M. P. van Dijk

Shell Research and Technology Centre Amsterdam, Postbox 38000, 1030 BN Amsterdam, The Netherlands

Received November 10, 1995; revised January 31, 1996; accepted February 29, 1996

Thin films (80–100 nm) of zinc titanate with Zn/Ti ratios between 0.5 and 2.7 were prepared on 2″ Si(100) wafers via the metallo-organic decomposition (MOD) technique. Their morphology, composition, and structure were extensively characterized by high resolution scanning electron microscopy, atomic force microscopy, X-ray photoelectron spectroscopy (XPS), Rutherford backscattering spectroscopy, energy dispersive X-ray analysis, secondary ion mass spectrometry (SIMS), X-ray diffraction (XRD), and glancing incidence XRD (GIXRD). The catalytic performance of these zinc titanate thin films in isobutane dehydrogenation was studied in a newly designed and built wafer reactor in the pulse mode. The zinc titanate films prepared via MOD consisted of irregularly shaped grains. The Zn/Ti ratio of the film surface as measured with XPS was slightly higher than that of the bulk, indicating some zinc enrichment on the surface. However, the overall composition through the film was reasonably homogeneous as revealed by a SIMS depth profiling study. GIXRD showed the existence of the same zinc titanate phases at all film depths, again indicating a homogeneous film. The zinc titanate phases found in the films depend primarily on the film stoichiometry. For films with a Zn/Ti ratio lower than 1, the phases found were zinc metatitanate ($ZnTiO_3$) with a hexagonal structure and titanium dioxide. In the films with a higher Zn/Ti ratio, the zinc titanate phase was $ZnTiO_3$ or Zn_2TiO_4, both possessing a cubic structure. Catalytic testing of these films in isobutane dehydrogenation showed a clear correlation between the structure and the catalytic performance. Zinc titanate phases with a cubic crystal structure were active for dehydrogenation, but the other phases were not. The most active catalyst has a Zn/Ti ratio close to 2, the stoichiometry of which corresponds to the Zn_2TiO_4 phase. The highest selectivity to isobutene was ca. 90 mol%, both at 823 and 923 K. The isobutane conversion was 2 and 8 mol%, respectively, at these two temperatures. Compared with the catalytic performance of a zinc titanate pellet pressed from powder material, the thin film catalyst exhibited a higher activity and a remarkably better stability.

INTRODUCTION

Catalytic dehydrogenation of isobutane to isobutene is an interesting route for providing additional olefin sources for the manufacture of methyl *tert*-butyl ether, which is required as an additive in reformulated gasoline by the "Clean Air Act." Thermodynamics indicate that in order to obtain a reasonably high conversion of the alkanes, the dehydrogenation process should be operated at elevated temperatures. In the current commercial or near-commercial dehydrogenation processes, the commonly applied catalysts are platinum or chromia systems supported on a carrier (mostly alumina) (1–3). These catalysts deactivate very quickly during the high temperature operation and need to be frequently regenerated (15–30 min to 2–7 days). In addition, the chromia-based catalyst is toxic, which causes environmental problems during operation (catalyst leaching) and during catalyst disposal. Hence, the development of new environmentally friendly catalytic systems offering better performance is of high interest.

In the literature, zinc titanate is reported to be active in the dehydrogenation of alkanes (4–6). Zinc titanate was first applied by Phillips Petroleum to the dehydrogenation of isobutane, resulting in a modest isobutene yield (4, 5). Recently, Lysova *et al.* (6) studied the effect of the chemical composition of the $ZnO–TiO_2$ catalytic system on its phase composition and catalytic properties in the oxidative and nonoxidative dehydrogenation of isobutane. It was found that samples with an atomic ratio of zinc to titanium ≥ 2 exhibited the highest selectivity with high specific activity. Zinc titanate is a material which is of low cost and environmentally friendly. These advantages of zinc titanate encouraged us to study this catalyst with the objective of determining whether there is a clear correlation between its composition/structure and performance and of gaining new leads for catalyst development.

An essential part of our strategy consisted of preparing zinc titanate catalysts in the form of thin films on 2″ silicon wafers, and using them in the direct (nonoxidative) dehydrogenation of isobutane to isobutene. Compared with conventional powder catalysts, thin film catalysts offer advantages of precise control of the catalyst (film) structure during preparation and easy access to various surface and bulk characterization techniques. The geometric configuration of a thin film catalyst is very different from a conventional powder catalyst. This results in very different mass transfer and diffusion behavior of the reactants, offering unique opportunities for research and application.

* To whom correspondence should be addressed.

0021-9517/96 $18.00

A large variety of techniques are available for the preparation of metal and metal oxide films (7). We applied the technique known as metallo-organic decomposition (MOD) (8) to prepare the zinc titanate thin films used in this work. MOD is a convenient technique for the preparation of thin films by liquid phase deposition. In the MOD preparation procedure, a precursor film was first prepared by spin-coating a flat substrate (e.g., a silicon wafer) with a solution containing the precursors, followed by the calcination of the precursor film to obtain a metal oxide film. Compared with the metallo-organic chemical vapor deposition technique we previously applied (9, 10), the MOD technique requires much simpler equipment. The preparation of zinc titanate films by the MOD technique is unknown in the literature, though the preparation of other titanates such as $BaTiO_3$ and $PbTiO_3$ has been reported (11–13). We used a precursor combination of zinc 2-ethylhexanoate and tetraisopropoxide titanium in an organic solvent for the preparation of the zinc titanate films. These two precursors are commonly used for the preparation of other thin films via MOD (12–14). The testing of these thin film catalysts requires a reactor with a different configuration from that used for powder catalysts. We built a quartz disk-shaped reactor (which we term a "wafer reactor") to test the catalysts at elevated temperatures. To minimize the gas phase thermal cracking reactions of isobutane, the wafer reactor was designed to have a very small void volume of ca. 0.6 ml. The catalysts were tested in pulse mode in order to avoid rapid catalyst deactivation at the high operating temperatures.

In this paper we demonstrate the possibility of preparing zinc titanate thin films on silicon wafers via MOD, and of studying the catalytic performance of these thin films in isobutane dehydrogenation.

EXPERIMENTAL

Thin films of zinc titanate on silicon wafers were prepared by first spin-coating a silicon wafer with the precursor solution to obtain a precursor-film, followed by a calcination procedure for the conversion into zinc titanate phases. The silicon wafers used have a diameter of 2″ and were cut in (100) orientation. They were purchased from Topsil. The precursor solution consisted of zinc 2-ethylhexanoate and tetraisopropoxide titanium (TPT) (both from Fluka) in *m*-xylene (HPLC grade, Aldrich). The typical concentration of the precursors in the coating solution was 12–14 wt% and 10–28 wt% for the titanium and zinc precursors, respectively. Zinc titanate thin films with different composition (Zn/Ti ratios between 0.5 and 2.7) were obtained by adjusting the composition of the precursor solution. A photoresist spinner from Headway Research Inc. was used for the spin-coating. The typically applied spin-coating conditions were 4000 rpm spin speed and 30- to 60-s spin time. The obtained precursor films were first dried at room temperature (RT) for 1 h and then calcined by the following procedure:

$$\mathrm{RT} \xrightarrow{1.7\ \mathrm{h}} 393\ \mathrm{K} \xrightarrow{2\ \mathrm{h}} 393\ \mathrm{K} \xrightarrow{8.8\ \mathrm{h}} 923\ \mathrm{K} \xrightarrow{2\ \mathrm{h}} 923\ \mathrm{K} \xrightarrow{\text{cooling (overnight)}} \mathrm{RT}.$$

Usually, two films were prepared consecutively under the same conditions. One of the two films was used for characterization purposes, while the other was subjected to the catalytic testing. Table 1 shows the typical preparation conditions and the basic properties of the prepared thin films. In most cases the two films prepared consecutively had a comparable weight uptake. Various analytical techniques revealed that they possessed a comparable structure and

TABLE 1

Preparation of Zinc Titanate Thin Films via the MOD Technique

	Coating solution			Zn/Ti[a]			
Sample	Zn-prec. (wt%)	Ti-prec. (wt%)	Film wt. (mg)	Coating solution	Film (XPS)	Film (RBS)	Cat. testing
S-1A	6.7	18.2	0.37	0.35	(0.54)	nd	Yes
S-1B	6.7	18.2	0.40	0.35	0.59	0.38	No
S-2A	7.0	13.3	0.72	0.50	nd	nd	Yes
S-2B	7.0	13.3	0.48	0.50	0.78	0.51	No
S-3A	15.8	15.1	0.27	1.0	(1.3)	nd	Yes
S-3B	15.8	15.1	0.32	1.0	1.3	0.96	No
S-4A	24.6	14.4	0.70	1.6	nd	nd	Yes
S-4B	24.6	14.4	0.69	1.6	1.9	1.6	No
S-5	27.5	14.7	0.90	1.8	2.0	1.7	No
S-6A	28.1	13.5	1.1	2.7	nd	nd	Yes
S-6B	28.1	13.5	nd	2.7	2.7	nd	No

[a] The values in parentheses are the Zn/Ti ratios of the films after catalyst testing. nd, not determined.

composition. Since it is more convenient to determine the weight uptake of the silicon wafers after film preparation than to measure the film thickness, the value of the film weight is given in Table 1. For reference, the 0.90 mg weight uptake of sample S-5 corresponds to a film thickness of 100 nm as measured in the high resolution scanning electron microscopy (HRSEM) images. To compare the catalytic performance of the thin film catalysts with those of the powder form, zinc titanate powder was prepared by drying the coating solution in a glass beaker, followed by a calcination procedure identical to that for the thin films.

Samples sent for characterization usually have a size of ca. 10×10 mm and are representative of the films. The actually analyzed areas are dependent on the analytical techniques and the conditions applied. The film composition, morphology and structure were characterized by various techniques. X-ray photoelectron spectroscopy (XPS) was carried out with a Kratos XSAM800 spectrometer, using Al$K\alpha$ radiation from a dual anode source, and the electrons were detected by a hemispherical analyzer in the fixed analyzer transmission mode. Dynamic secondary ion mass spectrometry (SIMS) was carried out on a Cameca IMS 4f with 8.0 keV Ar^+ primary ions. For taking high resolution scanning electron microscopy images a JEOL JSM-840A microscope was available which was equipped with energy dispersive X-ray analysis (EDX). Atomic force microscopy (AFM) images were taken with a Nanoscope II instrument from Digital Instruments. X-ray diffraction (XRD) was carried out with a Philips PW1820 goniometer using Cu$K\alpha$ radiation. Rutherford backscattering spectroscopy (RBS) and forward recoil spectroscopy (also known as elastic recoil detection) measurements were made at the Van de Graaff Laboratory at the University of Utrecht. The glancing incidence XRD (GIXRD) study was performed by Philips X-ray Analytical at Almelo, The Netherlands.

Catalytic testing of the thin film catalysts in isobutane dehydrogenation was performed in the pulse mode in a specially built wafer reactor. The reactor was constructed of two quartz plates joined leak-tight by a graphite film on the contact area. The center of the bottom plate contains a circular depression precisely cut to fit a wafer catalyst. An interstice between the top plate and the catalyst surface provides the space for reactant gas. This interstice was ca. 0.3 mm, resulting in a reactor void of ca. 0.6 ml. A schematic diagram of the quartz wafer reactor is presented in Fig. 1. The reactor can be operated under atmospheric pressure up to a temperature as high as 973 K. The gas flow pattern and the temperature profile over the reactor under operating conditions (atmospheric, 923 K) were simulated by applying the commercially available computational fluid dynamics (CFD) package Harwell Flow 3D. A more sophisticated and advanced simulation study is continuing and details of the results will be published later (15). The initial simulation results show that the distribution of gas velocity over the wafer surface is reasonably uniform and that the reactant gas reaches the reactor temperature almost immediately upon entering the reactor.

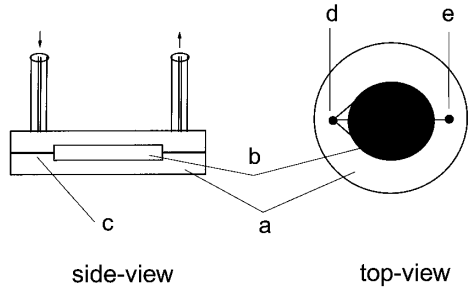

FIG. 1. Schematic drawing of the quartz wafer reactor. a, quartz plate; b, reactor void for a thin film catalyst; c, graphite ring; d, gas inlet; e, gas outlet.

For representative GC-sampling in pulse mode testing, it is crucial that the block shape of the pulses is preserved after passing through the reactor. Figure 2 shows the shape of two pulses (N_2 in Ar) after passing through the reactor. The gas volume of the two pulses was 2 and 5.7 ml, corresponding to a ratio of pulse/reactor void of 3.3 and 5, respectively.

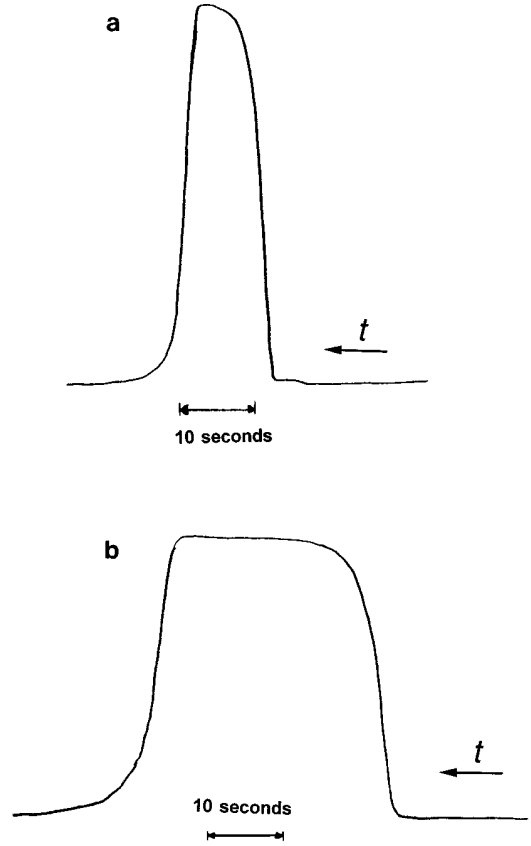

FIG. 2. Shape of a pulse (N_2 in Ar) after passing through the reactor with a pulse volume of 2 ml (a) and 5.7 ml (b).

It is evident that acceptable block-shaped pulses with a sufficiently long, flat part can be obtained if the pulse/reactor void volume ratio is larger than 5. During catalytic testing the gas volume of each pulse was 5.7 ml.

The feedstock was isobutane diluted with nitrogen to a concentration of 1.7, 22, and 34 vol%. The gas flow rate was 0.58 normal liter/h. The products were split into two parts, and both were analyzed by GC. One part was passed over an Al_2O_3/Na_2SO_4 column connected to a flame ionization detector (FID) for the analysis of C_1–C_5 hydrocarbons. The other part was passed over a Poraplot Q column to separate H_2, N_2, CO, and CO_2 under cryogenic conditions. These gases were detected by means of a thermal conductivity detector (TCD). The calculation of the isobutane conversion and the selectivity to isobutene were based on the carbon mass balance. The calculation of isobutane conversion and selectivity to isobutene were made using Eqs. [1] and [2], respectively. These equations are valid only when no significant coke deposition occurs on the catalysts, which was the case in the current study.

$$X_{\mathrm{IB}} = \frac{\sum n \cdot C_{n,i} - 4 \cdot C_{\mathrm{IB}}}{\sum n \cdot C_{n,i}} 100\% \qquad [1]$$

$$S_{\mathrm{IBE}} = \frac{4 \cdot C_{\mathrm{IBE}}}{\sum n \cdot C_{n,i} - 4 \cdot C_{\mathrm{IB}}} 100\%, \qquad [2]$$

where

X_{IB},	isobutane conversion (mol%)
S_{IBE},	isobutene selectivity (mol%)
n,	number of carbon atoms in component i
$C_{n,i}$,	mole percentage of component i in product
C_{IB},	mole percentage of (unconverted) isobutane in product
C_{IBE},	mole percentage of isobutene in total product.

RESULTS

Characterization of the Zinc Titanate Thin Films

We applied several analytical techniques to characterize zinc titanate thin films with respect to film morphology, composition, and structure. These properties are often closely related to the catalytic performance in heterogeneous catalysts. The surface of the zinc titanate films prepared via the MOD technique is relatively smooth over a large area (Fig. 3a, Zn/Ti = 2.0). Under a higher magnification, a film structure consisting of irregularly shaped, packed grains can be observed (Fig. 3b). Figure 4 shows the HRSEM image of a side-edge of the film, from which the thickness of the film can be determined. A structure of compacted grains can again be identified. An AFM image of this sample is shown in Fig. 5. The morphology observed by AFM is consistent with that observed by HRSEM. Zinc titanate films with different Zn/Ti ratios possess a slightly different morphological structure. With a decrease in the Zn/Ti ratio, the distribution of the grain sizes becomes bimodal. Some larger grains are observed in addition to the usual ones. Figure 6 shows a HRSEM image of a zinc titanate film with Zn/Ti = 0.78.

We applied XPS to determine the surface composition of the thin films. XPS is a surface sensitive technique which determines the composition of the outermost 2- to 3-nm surface layer. Unless otherwise specified, the Zn/Ti ratios presented in this paper are the values measured by XPS. To check the consistency of the film composition on the surface and in the bulk, we applied the RBS and EDX techniques to determine the bulk composition. For a film with a surface Zn/Ti ratio of 2.0, the Zn/Ti ratios determined by RBS and EDX were 1.7 and 1.8–1.9, respectively. These values are slightly lower than those of the surface composition, suggesting that the surface layer of the film contains more zinc than the deeper part. However, the subsurface film composition was reasonably homogeneous, as revealed by a SIMS depth profiling study. Figure 7 shows the dynamic SIMS depth profile of a zinc titanate film having a surface Zn/Ti ratio of 1.9. With increasing depth into the film, the titanium signal remains relatively constant, while that of zinc decreases slightly. The considerable change of the intensity at the beginning of profiling is partly due to the instability of the yield of secondary ions, which is a common phenomenon observed in SIMS depth profiling (16). On the other hand, the observed profile also suggests that the Zn/Ti ratio of the film surface is higher than that of the bulk, in agreement with the combined results of the XPS, RBS, and EDX measurements. For other zinc titanate films there is also some zinc enrichment on the surface, since the Zn/Ti ratios measured by XPS (surface composition) are usually higher than those measured by RBS (bulk composition) as can be seen from Table 1.

The crystal structures of a series of zinc titanate films having different Zn/Ti ratios were studied by applying the normal XRD technique. Two of these samples were also studied by the GIXRD technique. The normal diffraction pattern of the sample with a Zn/Ti of 2.0, together with the standard line pattern of Zn_2TiO_4 (JCPDS [25-1164]) is shown in Fig. 8. The huge peak at $2\Theta = 70^\circ$ stems from the wafer substrate. The good agreement of these two diffraction patterns suggests that the zinc titanate phase in this sample is mainly Zn_2TiO_4. Table 2 lists the phases identified in zinc titanate films with different Zn/Ti ratios. A clear difference exists between the phases found in the films with a Zn/Ti ratio lower than 1 and those with a higher ratio. For the films with a ratio of Zn/Ti < 1, TiO_2 (rutile and/or anatase) and hexagonal $ZnTiO_3$ [26-1500] phases were found, while for films with a ratio of Zn/Ti > 1, the phases found were cubic zinc titanates ($ZnTiO_3$ [39-190] or Zn_2TiO_4 [25-1164]). From the compositional formulation,

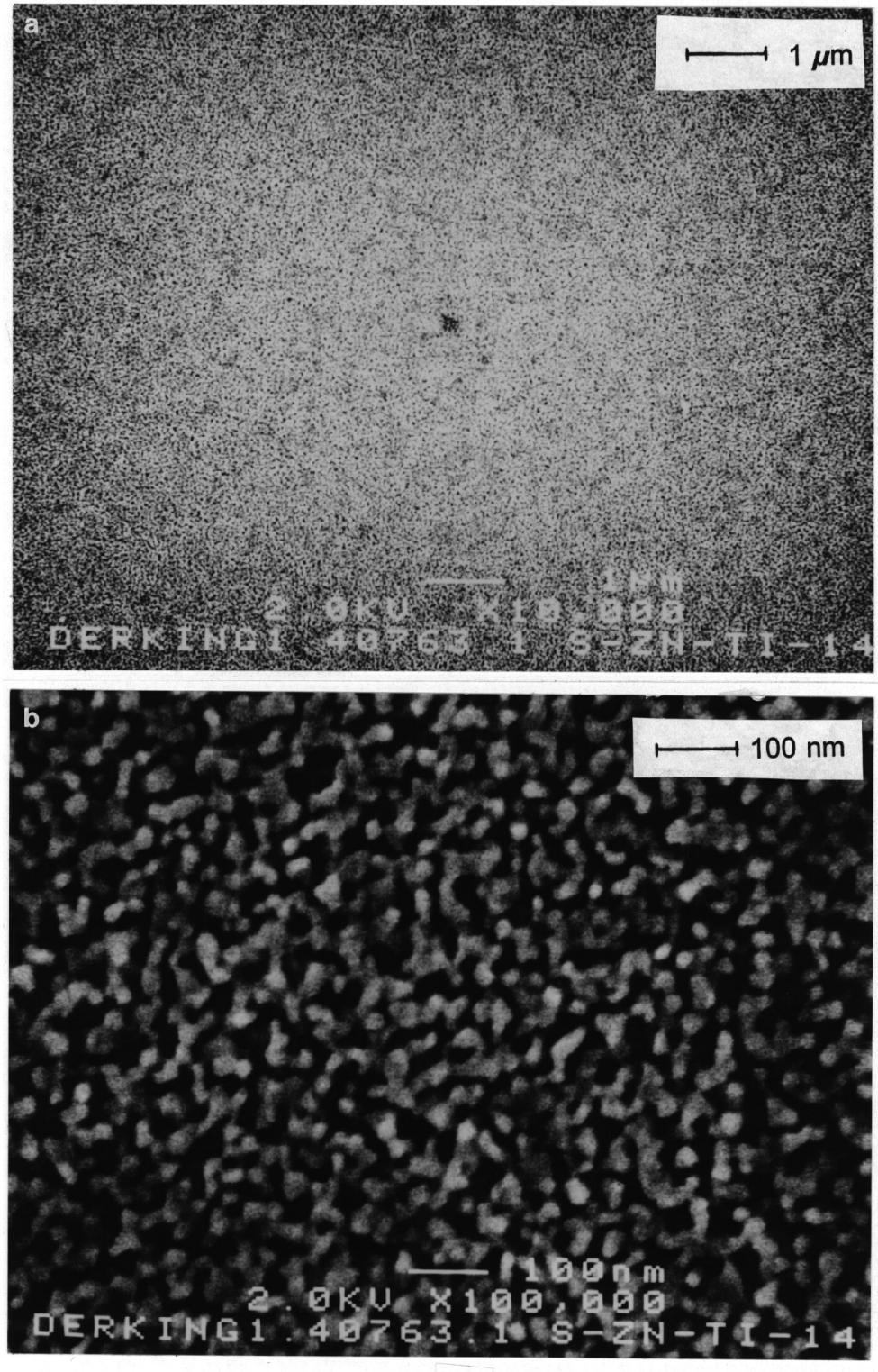

FIG. 3. HRSEM images of a zinc titanate thin film with Zn/Ti = 2.0.

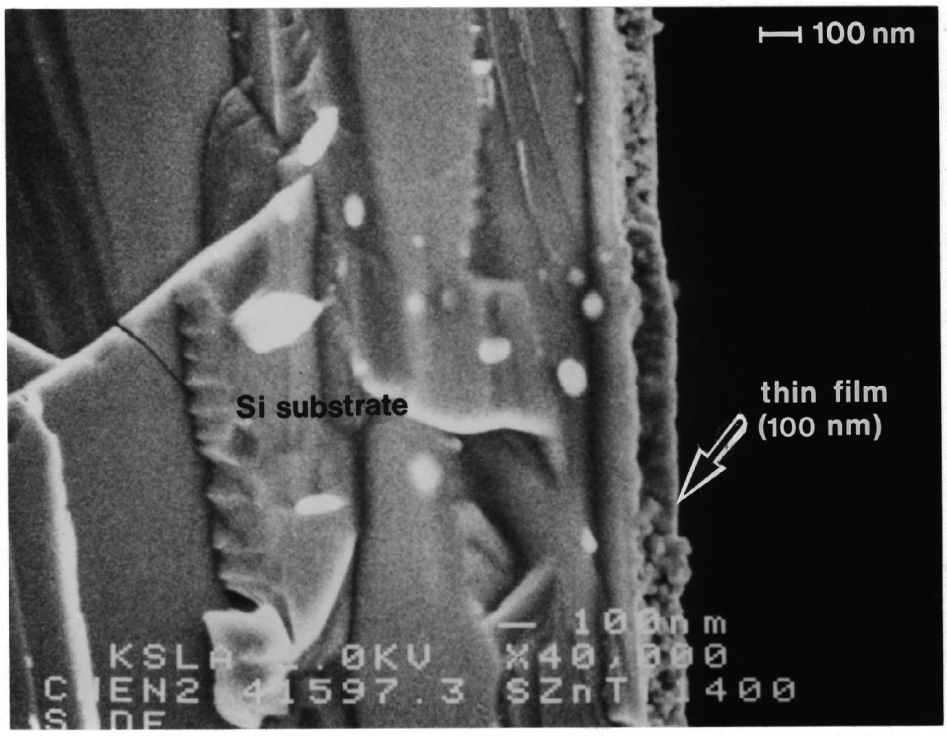

FIG. 4. HRSEM image of the side-edge of a zinc titanate thin film (Zn/Ti = 2 .0).

sample S-6B (Zn/Ti = 2.7) should contain a phase rich in zinc (e.g., ZnO) in addition to the Zn_2TiO_4 phase. However, no other phase was found in the XRD study, possibly due to the extra zinc species being finely dispersed in the film.

The results of phase identification obtained above were further supported by applying the GIXRD technique to two of the zinc titanate films with a Zn/Ti ratio of 2.0 and 0.59, respectively. Figure 9 shows the diffraction patterns of the sample with Zn/Ti = 2.0 recorded with incident angles of 0.25°, 0.5°,1.0°, and 2°. It is clear that the quality of the diffractograms recorded in the glancing incidence mode is superior to those recorded with the normal diffraction technique. In the GIXRD patterns the huge Si(100) reflection ($2\Theta = 69.13°$) is absent, as are the ghost lines in conjunction with this line. With the help of database references, the presence of zinc orthotitanate Zn_2TiO_4 [25-1164] was identified for this sample, which confirms the conclusion of the normal XRD study. The diffraction pattern of this sample does not change with the angle of incidence, suggesting a homogeneous phase through the bulk of the film. For the sample with a Zn/Ti ratio of 0.59, three phases were observed, namely zinc metatitanate $ZnTiO_3$ (hexagonal, [26-1500]), and TiO_2 in both the rutile [21-1276] and anatase [21-1272] structural variants. This is also in agreement with the observations from the normal diffraction study, but with a much higher level of confidence. The diffraction pattern of this sample does not vary with Θ_i, suggesting that the same phases exist at different depths within the film.

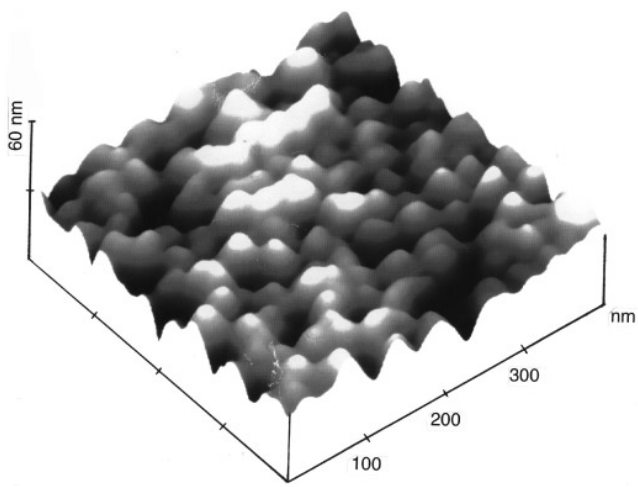

FIG. 5. AFM image of a zinc titanate thin film with Zn/Ti = 2.0.

Catalytic Performance of Zinc Titanate Thin Films

Before testing the zinc titanate thin films, the background activity of the wafer reactor was determined. The reactor was filled with a bare silicon wafer to ensure a comparable gas flow pattern when testing the film catalysts. The feedstock consisted of 1.7 vol% isobutane in nitrogen. The choice of a low concentration of isobutane in the feedstock

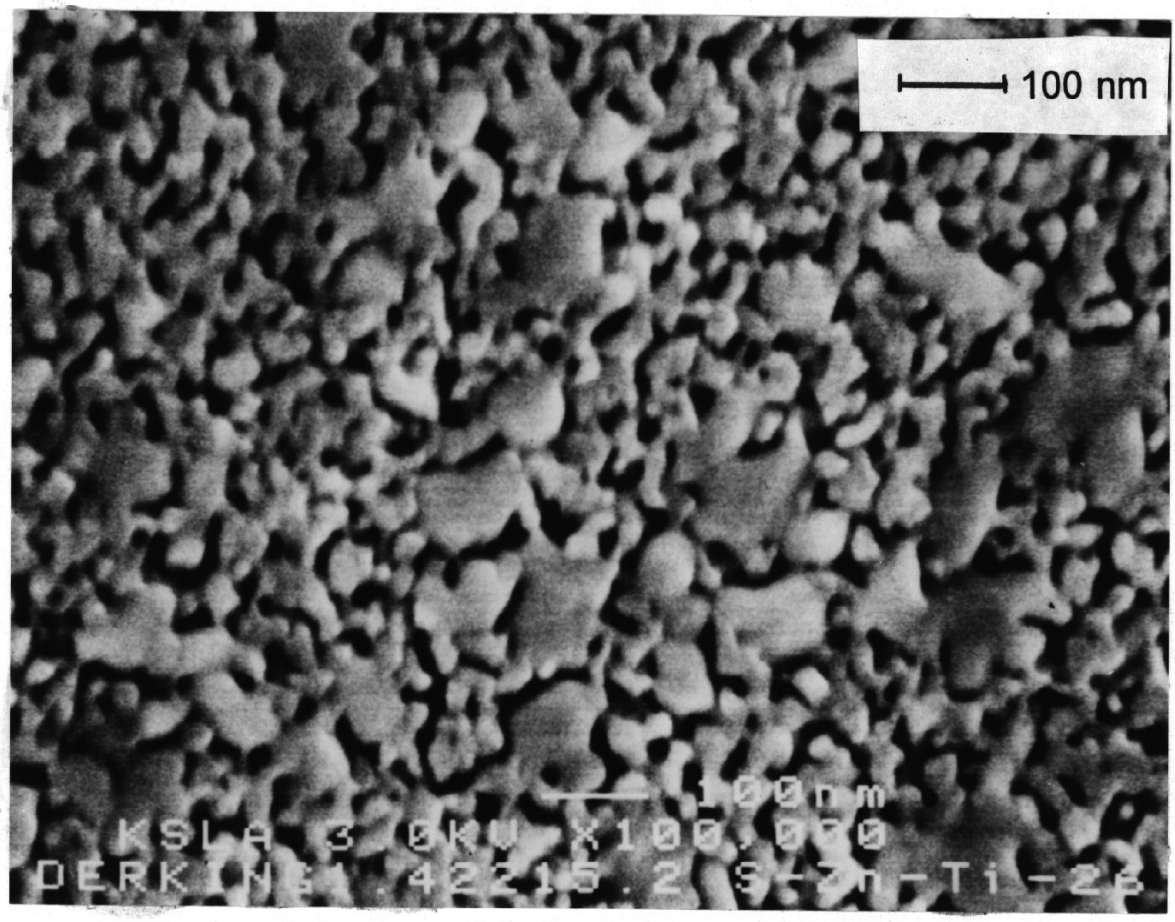

FIG. 6. HRSEM image of a zinc titanate film with a Zn/Ti ratio of 0.78.

was based on the consideration that the total surface area of the thin film catalysts was very low, so that a high isobutane concentration might make it difficult (a) to detect the products in low concentration and (b) to obtain sufficient data before the catalysts were deactivated. The conversion of isobutane was 0.3 and 3.1 mol% at 823 and 923 K, respectively, and the selectivity to isobutene was 72 and 60 mol%. The background activity of the wafer reactor has a threefold origin, namely, the surface reactions of isobutane on the silicon wafer and on the quartz reactor wall and the thermal gas phase reaction. In thin film catalysts, the upper part of the silicon wafer is covered with a layer of catalytic material, so that the actual "background activity" during catalytic testing should be smaller than the values obtained above.

A series of zinc titanate films with different Zn/Ti ratios was then tested during isobutane dehydrogenation at 823 and 923 K. For comparison, the catalytic performances of a ZnO and TiO_2 thin film were also determined. The main byproducts of the high temperature isobutane dehydrogenation reaction were methane, propene, and, to a lesser amount, butadiene. The remaining components were ethene, *n*-butenes, and *n*-butane. Figure 10 shows the dependence of product selectivity on the catalyst composition at 823 and 923 K. To keep the selectivity of isobutene consistent through the text, the product selectivity in Fig. 10 is presented in percentage of mole carbons instead of mole molecules. The values given are the average data of the first five to eight pulses during the testing. The isobutane conversion at these two temperatures is shown in Fig. 11. The conversions of isobutane at 923 K are higher than those at 823 K. At 923 K, the cracking reaction of isobutane is much more significant than that at 823 K, leading to the formation of a considerable amount of methane and propene. For zinc titanate films with a Zn/Ti ratio between 1.3 and 2.7, both the conversion of isobutane and the selectivity to isobutene were significantly higher than the background of the reactor and those found in the other films. From the XRD study (Table 2) we know that zinc titanate films with a Zn/Ti ratio higher than unity possess a cubic structure. This and the catalytic testing results led us to conclude that zinc titanates with a cubic crystal structure are active in the dehydrogenation reaction.

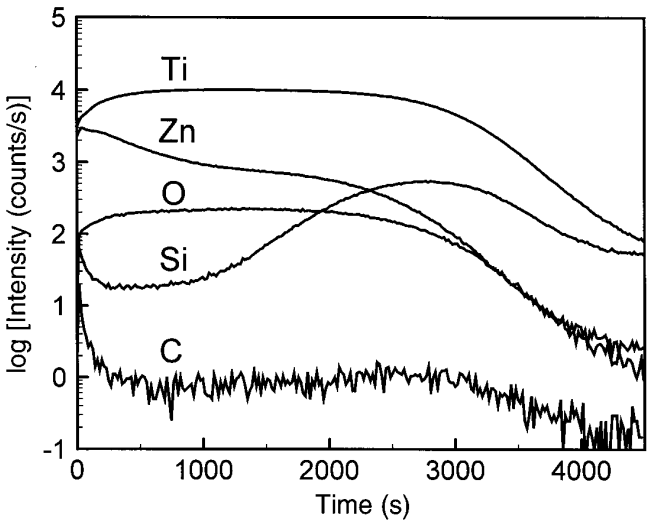

FIG. 7. SIMS depth profile of a zinc titanate film on a silicon wafer with Zn/Ti = 1.9.

Comparison of the Performances of Thin Film and Powder Catalysts

To compare the catalytic performance of the thin film catalysts with that of the powder form, we also tested a zinc titanate powder, prepared via the MOD technique, in isobutane dehydrogenation. This powder form zinc titanate catalyst has a surface composition of Zn/Ti = 2.0. XRD showed that the main phase was Zn_2TiO_4 with a cubic structure. The powder catalyst was pressed into a pellet (diameter, 15 mm; thickness, ca. 0.5 mm) before being tested in the wafer reactor. The amount of zinc titanate in the pellet catalyst was 29.5 mg, while that of the thin film catalyst was 0.55 mg. The feedstock used was 34 vol% isobutane in nitrogen for the first three pulses and then 22 vol% for the remaining pulses. The purpose of switching the feed gas to a lower isobutane concentration after three pulses was to retard the catalyst deactivation rate so that more data could be collected. Figure 12 shows the dependence of isobutane conversion and the selectivity to isobutene on the number of pulses for these two catalysts. The powder catalyst showed a slightly higher initial conversion rate than that of the thin film catalyst. However, both the conversion of isobutane and the selectivity to isobutene over the powder catalyst decreased very quickly with the given pulses, while the performance of the thin film catalysts remained stable. The selectivity to isobutene with the thin film catalyst remained relatively constant at close to 90 mol%. The results show that the thin film catalyst exhibited a remarkably improved stability. In addition, it is important to note that the amount of the zinc titanate material in the thin film catalyst was much less than that of the powder catalyst, indicating that either the thin film catalyst is more active or its efficiency is much higher.

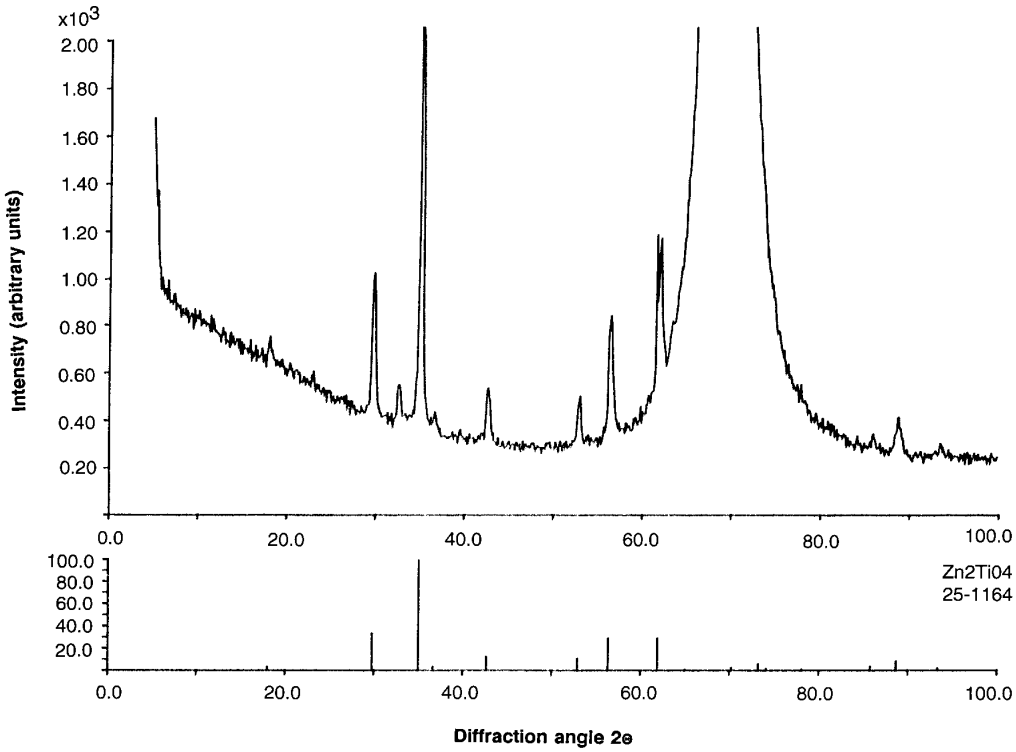

FIG. 8. XRD diffraction pattern of a zinc titanate thin film with Zn/Ti = 2.0.

TABLE 2

Phase Identification of Zinc Titanate Films with Different Zn/Ti Ratios

Sample	S-1B	S-2B	S-3B	S-5	S-6B
Zn/Ti (XPS)	0.59	0.78	1.3	2.0	2.7
Phases identified [JCPDS]	TiO_2 (r) [21-1276] TiO_2 (a) [21-1272] $ZnTiO_3$ (h) [26-1500]	TiO_2 (r) [21-1276] $ZnTiO_3$ (h) [26-1500]	$ZnTiO_3$ (c) [39-190]	Zn_2TiO_4 (c) [25-1164]	Zn_2TiO_4 (c) [25-1164]
Main phase	$ZnTiO_3$ (h)	$ZnTiO_3$ (h)	$ZnTiO_3$ (c)	Zn_2TiO_4 (c)	Zn_2TiO_4 (c)

Note. a, anatase; r, rutile; h, hexagonal; c, cubic.

DISCUSSION

We have prepared zinc titanate thin films and studied their catalytic performance in isobutane dehydrogenation. Compared with the conventionally applied powder form catalysts, thin film catalysts have significant advantages with regard to catalyst characterization and the determination of the relation between structure and catalytic performance. In the powder form catalysts, the inhomogeneous morphology and the complexity of the structure often make an exact characterization difficult. For thin film catalysts, the quasi-two-dimensional structure allows the application of many surface and bulk analytical techniques which provide a clear picture concerning the film morphology, the surface/bulk composition, and the structure. The zinc titanate thin film catalysts possessed a homogeneous morphology. The composition throughout the thickness of the film was uniform, as suggested by the reasonable agreement between the surface and bulk Zn/Ti ratios as well as by the SIMS study. In the SIMS depth profiling, the appearance of the silicon signal occurred earlier than expected. This is not due to the formation of silicate phases but can be explained by the fact that the film consist of compacted grains. The sputtering beams can thus reach the silicon substrate between the grains at an early stage, before all of the zinc titanate material is sputtered away. The GIXRD results proved that the zinc titanate thin films possessed the same phases throughout the film depth for the samples with a Zn/Ti ratio of

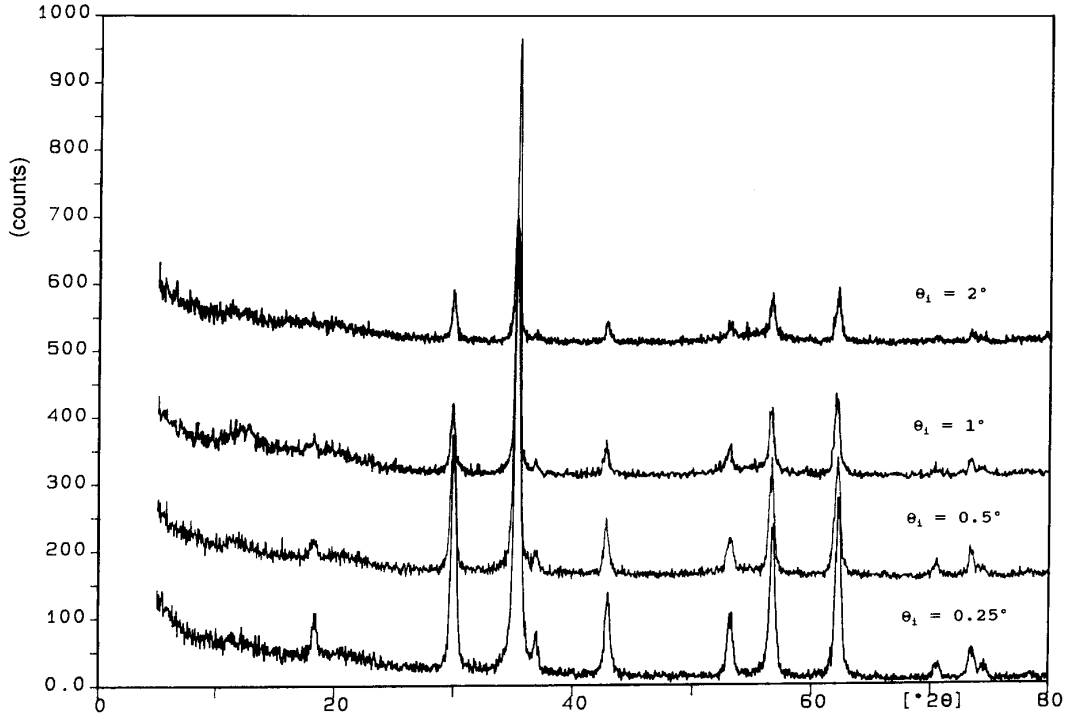

FIG. 9. Glancing incidence X-ray diffraction patterns for Θ_i equal to 0.25°, 0.5°, 1°, and 2°, respectively. Zn/Ti = 2.0.

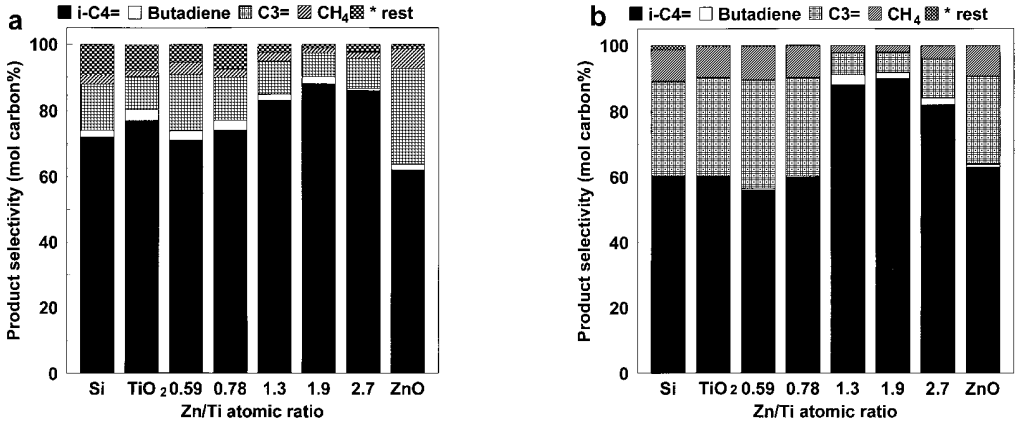

FIG. 10. Dependence of product selectivity in isobutane dehydrogenation on the film composition. (a) 823 K, (b) 923 K. * rest represents ethene, *n*-butenes, and *n*-butane.

2.0 and 0.59. No phases consisting of silicon with zinc or titanium were found, indicating that no reaction occurred between the zinc titanate phases and the silicon substrate.

In connection with the assignment of zinc titanate phases, it is worth discussing the phase diagrams and crystal structures of the zinc titanate system in more detail. In the literature, the existence of several zinc titanate phases with different structures is reported; however, some of these compounds do not coincide with each other in different reports. Table 3 provides an overview of the various zinc titanate phases and the corresponding structures reported in the literature. The formation of the hexagonal-form zinc metatitanate ($ZnTiO_3$) and the cubic-form zinc orthotitanate (Zn_2TiO_4) phases is well documented (17–21), while the existence of the cubic $Zn_2Ti_3O_8$ phase remains somewhat uncertain. The assignment by Bartram and Slepetys (18) (JCPDS reference [13-471]) was replaced by an assignment by Reddy *et al.* (20) [38-500] with fewer diffraction lines, and Yamaguchi *et al.* (21) suggested that the earlier pattern was in fact due to a cubic $ZnTiO_3$. We assign the main zinc titanate phase found in the sample with a Zn/Ti ratio of 1.3 as cubic $ZnTiO_3$ on the basis of the suggestion by Yamaguchi *et al.* (21), though the Zn/Ti atomic ratio of this phase (Zn/Ti = 1) is lower than that of the surface composition (Zn/Ti = 1.3). The diffraction pattern of the Zn_2TiO_4 phase in this work is comparable to that of the standard JCPDS pattern of [25-1164] rather than that of the other standards [18-1487], [19-1483], and [30-1493].

From the correlation found between catalyst structure and catalytic performance we conclude that zinc titanates with a cubic structure are active in the dehydrogenation of isobutane. This conclusion is in agreement with the work

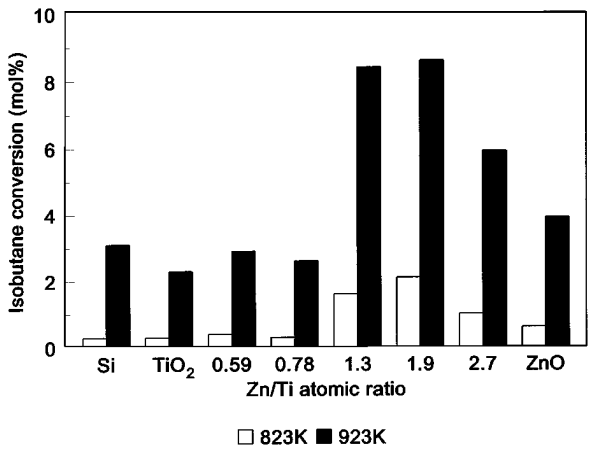

FIG. 11. Dependence of isobutane conversion on the catalyst composition at 823 and 923 K.

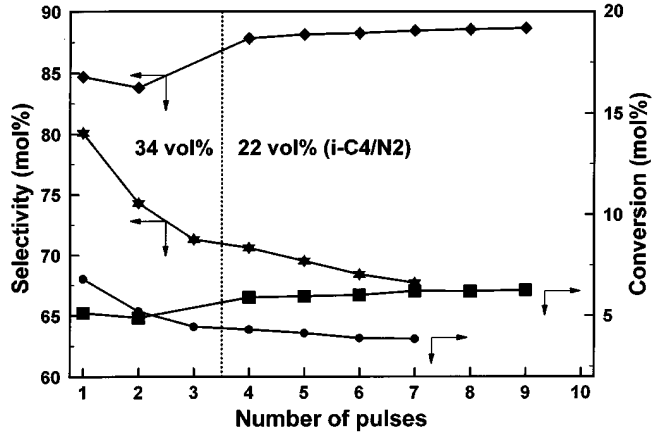

FIG. 12. Comparison between the performances of zinc titanate thin film (Zn/Ti = 1.9) and the powder form (Zn/Ti = 2.0) catalysts in isobutane dehydrogenation at 923 K. Isobutane conversion with the thin film (■) and powder (●) catalysts. Selectivity to isobutene with the thin film (◆) and the powder (★) catalysts.

TABLE 3

Zinc Titanate Phases and the Crystal Structures Reported in the Literature

	Zn_2TiO_4	$ZnTiO_3$	$ZnTiO_3$	$Zn_2Ti_3O_8$
Name	Ortho zinc titanate	Meta zinc titanate	Meta zinc titanate	
Structure type	Inverse spinel	Ilmenite		Spinel-like
Symmetry	Cubic	Hexagonal/ Rhombohedral	Cubic	Cubic
Spacegroup	Fd3m	R3	Fd3m	Fd3m
Unit cell	$a = 8.456$ Å (18) $a = 8.445$ Å (19) $a = 8.449$ Å (20)	$a = 5.49$ Å $\alpha = 55.10^\circ$ (18)	$a = 8.408$ Å (21)	$a = 8.395$ Å (18) $a = 8.429$ Å (20)
Zn/Ti ratio	2.0	1.0	1.0	0.67
Atomic position	Zn in 8a Zn in 16d, 50% Ti in 16d 50%			Zn in 8a Ti in 16d, 75%

of Lysova *et al.* using zinc titanate powder catalysts (6). The overall understanding as to why zinc titanates with a cubic structure are active in dehydrogenation is still very poor and needs to be further investigated. The structural differences between the hexagonal and cubic zinc titanates include the coordination number of the metal atoms and the interatomic distances. The hexagonal zinc metatitanate belongs to space group R3 with 2 molecules in the primitive rhombohedral cell. All the Zn atoms are in octahedral coordination with oxygen. The cubic zinc titanates are of the (inverse) spinel type or related to that structure. In the cubic zinc orthotitanate (Zn_2TiO_4), all the 8a positions (tetrahedrally surrounded) are occupied by Zn atoms, and of the 16d positions (octahedrally surrounded) half are occupied by zinc and the other half by titanium. The interatomic distances for these two types of zinc titanates are also different. Table 4 lists the interatomic distances in zinc titanates, zinc oxide, and titanium dioxide. For the two cubic zinc titanates Zn_2TiO_4 and $ZnTiO_3$, the interatomic distances between Zn and Zn,Ti and Ti, Zn and Ti, Zn and O, and Ti and O are comparable. However, some of these values differ significantly from those of the hexagonal zinc metatitanate, $ZnTiO_3$. It can be speculated that the structural difference between the two types of zinc titanates will influence the interaction with isobutane and subsequently result in different catalytic performance. However, the complexity of the system involved and the very limited information available do not allow a clear picture as to how this difference has resulted in different catalytic performance.

TABLE 4

Interatomic Distances (in Å) in Zinc Titanates, Zinc Oxide, and Titanium Dioxide

	Zn–Zn	M–M	O–O	Zn–M	Zn–O	M–O
Zn_2TiO_4 Cubic [25–1164]	3.66	2.99	3.28 (Zn) 3.00 (M) 4.04 (M)	3.51	2.01	2.02
$ZnTiO_3$ Cubic [39–190]	3.64	2.97	2.69 (Ti) 3.26 (Zn)	3.49		2.01
$ZnTiO_3$ Hexagonal [26–1500]	3.93	2.97 4.18	3.09 (Zn) 2.64 (Ti)	3.41 2.91	1.96	2.06 2.01
ZnO (Zincite) (Ref. 18)	3.20 3.24		3.20 3.24		1.97	
TiO_2 Rutile (Ref. 18)		2.98	2.78 2.53			1.95 1.98

Note. M, octahedral site.

Another advantage of using thin film catalysts, at least in the current case, is that they are more active and stable. We suggest that this is a result of the different geometries of the thin film and the powder catalysts. In the high temperature catalytic dehydrogenation process, coke formation is often one of the main causes of catalyst deactivation. To check whether coke formation could also cause catalyst deactivation for zinc titanates, we deactivated a zinc titanate thin film catalyst by passing a large amount of pure isobutane over the film at 923 K. Analysis of this deactivated film by the forward recoil spectroscopy technique revealed that the concentration of carbon in the deactivated sample (4.9×10^{16} atoms/cm^2) was significantly higher than that of the fresh sample (1.2×10^{16} atoms/cm^2). Coke formation on catalysts is usually caused by the oligomerization and polymerization of olefinic species. For the thin film catalyst, the diffusion path of the olefinic products formed over the catalyst is shorter, and the olefin flux through the outermost catalyst layer is lower than that of the pressed pellet catalyst under the currently applied reactor configuration. This could have resulted in a slower coke formation in the thin

film catalysts. To ensure that the quick deactivation of the powder catalyst is not due to an artificial effect of pressing the catalyst into a pellet form, we also tested the catalyst in the powder form in a tube reactor (ID = 1 mm) under otherwise the same conditions. This catalyst also deactivated quickly under the pulses employed.

CONCLUSION

A novel research route for studying catalytic reactions has been applied by preparing and testing thin film catalysts. The wafer reactor configuration used in this work proved to be successful for the testing of catalytic reactions at elevated temperatures in the pulse mode. The quasi-two-dimensional structure of the thin film catalysts, and their accessibility to a wide variety of surface and bulk analysis techniques enabled us to characterize exactly the catalyst surface and bulk composition and structure. The zinc titanate films prepared by the MOD technique possess a uniform composition and structure throughout the film. Zinc titanates with a cubic structure are the only active phases in isobutane dehydrogenation. The thin film catalysts exhibit a higher activity and a remarkably better stability than the powder form catalyst. The application of these thin film catalysts in practical operation needs to be further explored.

ACKNOWLEDGMENTS

The authors thank G. M. Mulder for the XPS measurements, C. van der Spek for taking SIMS depth profiles, J. B. van Mechelen for carrying out part of the XRD work, N. Groesbeek for the HRSEM images, R. van den Berg for the AFM images, and H. Wang for performing the CFD simulation. We thank Philips X-ray Analytical at Almelo for the GIXRD work.

REFERENCES

1. Catalytica Studies Division, "Catalytic Dehydrogenation and Oxidative Dehydrogenation," Catalytica Study 4190 DH. 1991.
2. Catalytica Studies Division, "Oxidative Dehydrogenation and Alternative Dehydrogenation Processes," Catalytica Study 4192 OD. 1993.
3. Resasco, D. E., and Haller, G. L., *in* "Catalysis," Vol. 11, p. 379. Royal Society of Chemistry, 1994.
4. Esstman, A. D., and Okla, B. (Phillips Petroleum Company), U.S. patent 4,327,238 (1982).
5. Aldag, A. W., and Okla, B., U.S. patent 4,524,144 (1985).
6. Lysova, N. N., Tmenov, D. N., and Luk'yanenko, V. P., *J. Appl. Chem. USSR* **65**, 1500 (1993). [Translated from *Zh. Prikl. Khim.* **65**, 1848–1855 (1992)].
7. Schuegraf, K. K. (Ed.), "Handbook of Thin-Film Deposition Processes and Techniques, Principles, Methods, Equipment and Applications." Noyes Publications, Park Ridge, NJ, 1988.
8. Hanrahan, J. R., Sanchez, E., Santiago, J. J., Berry, D. H., and Jiang, Q., *Thin Solid Fllms* **202**, 235 (1991).
9. Chen, Z. X., and Derking, A., *J. Mater. Chem.* **3**, 1137 (1993).
10. Chen, Z. X., van der Eyden, J., Koot, W., van den Berg, R., van Mechelen, J., and Derking, A., *J. Am. Ceram. Soc.* **78**, 2993 (1995).
11. Shaikh, A. S., and Vest, G. M., *J. Am. Ceram. Soc.* **69**, 682 (1986).
12. Wang, Y., Zhang, P., Qu, B., and Zhong, W., *J. Appl. Phys.* **71**, 6121 (1992).
13. Faure, S. P., Barboux, P., Gaucher, P., and Livage, J., *J. Mater. Chem.* **2**, 713 (1992).
14. Jean, J. H., *J. Mater. Sci. Lett.* **9**, 127 (1990).
15. Derking, A., Chen, Z. X., *et al.,* to appear.
16. Benninghoven, A., Rudenauer, F. G., and Werner, H. W., "Secondary Ion Mass Spectrometry" Wiley, New York, 1987.
17. Dulin, F. H., and Rase, D. E., *J. Am. Ceram. Soc.* **43**, 125 (1960).
18. Bartram, S. F., and Slepetys, R., *J. Am. Ceram. Soc.* **44**, 493 (1961).
19. Verwey, E. J. W., and Heilman, E. L., *J. Chem. Phys.* **15**, 174 (1947).
20. Reddy, V. B., Goel, S. P., and Mehrotra, P. N., *Mater. Chem. Phys.* **10**, 363 (1984).
21. Yamaguchi, O., Morimi, M., Kawabata, H., and Shimizu, K., *J. Am. Ceram. Soc.* **70**, C-97 (1987).